Applied Computer Science 2025, vol. 21, no. 3, pp. 59–71
https://doi.org/10.35784/acs_7340

Submitted: 2025-02-25 | Revised: 2025-05-15 | Accepted: 2025-06-01

Keywords: solder joint failure, impact loading, peel stress, finite element methods, ensemble methods

Venkata Naga Chandana YAGNAMURTHY [1], *Venu Kumar NATHI* [1*]
[1] GITAM University, India, chandana.svn@gmail.com, vnathi@gitam.edu
[*] Corresponding author: chandana.svn@gmail.com

A machine learning approach for evaluating drop impact reliability of solder joints in BGA packaging

Abstract

The failure of solder joints of Ball Grid Array (BGA)Package under drop impact is influenced by multiple parameters, highlighting the need for optimization during the early design stages of electronic systems. In this paper, ensemble methods were developed to predict failure in solder joints by estimating the dynamic responses of printed circuit board assembly (PCBA) during drop impact conditions. Finite element (FE) simulations were carried out by varying PCB thickness, PCB modulus, solder ball diameter, and solder ball material to obtain the dynamic responses of the PCBA during impact loading, which served as the dataset for the predictive model. Also drop test experiments were conducted according to the JESD22-B111A standard to validate the FEM results. XGBoost regression achieved the best performance with an R^2 of 0.96 and the lowest error, with feature importance analysis identifying solder ball material (score: 0.447) as the most influential factor and PCB modulus (score: 0.065) as the least.The predictive model developed in this work offers a robust tool for evaluating mechanical performance and optimizing design parameters in PCBA structures under dynamic mechanical stresses.

1. INTRODUCTION

Advances in hardware technology have enabled the development of smaller, high-density electronic chips. Solder joints play a critical role in these devices, providing both mechanical support and electrical connectivity between the printed circuit board (PCB) and the chip. With miniaturization, ensuring the reliability of solder joints is critical, as they are exposed to thermal cycling, high electrical currents, vibration, and drop impacts. Since portable devices are prone to accidental drops, assessing their durability is critical (Gu et al., 2018). A board-level drop test method is commonly used to evaluate the robustness of electronic assemblies under drop impacts (JEDEC, 2024). Numerous experimental and simulation-based studies have evaluated the performance of solder joints under drop conditions according to JEDEC-B111 standards (Muthuram & Saravanan, 2022). The primary cause of solder joint failure is tensile stress, also referred to as peel stress , which results from the stiffness mismatch between the PCB and the BGA (Gu et al., 2017). Several factors affect the long-term reliability of solder joints, including copper pad size, underfill material, solder ball properties, PCB characteristics, component placement, and solder ball geometry (Wang et al., 2021). Finite element (FE) analysis has been widely used to evaluate the reliability of lead-free solder in thin fine-pitch ball grid array (TFBGA) packages under various stress conditions. Research results indicate that strain rate significantly affects the stress distribution, while temperature variations change the location of the maximum stress (Niu et al., 2015). However, most of these studies have mainly focused on strain rate and temperature effects, while other critical factors influencing solder joint reliability under drop impact conditions remain underexplored.

Previous studies have shown that solder joint failure tends to follow a lognormal distribution, with the highest stress concentrations observed in the outermost solder balls, leading to crack initiation near the intermetallic compound (IMC) layer (Chen et al., 2020; Xia et al., 2017). Several approaches, including experimental methods, simulations, and machine learning (ML) techniques, have been employed to predict solder joint failure under various conditions (Apalowo et al., 2024; Arriola et al., 2023; Tee et al., 2004; Wu et al., 2018).

ML models are increasingly used in electronic packaging research because of their ability to analyze complex, nonlinear relationships. AI-based techniques help establish relationships between design parameters, operating conditions, and performance results (Yuan et al., 2024). Neural network-based models have been

used to predict solder joint life under drop conditions by taking into account multiple influencing factors such as BGA chip location and solder ball volume, achieving high prediction accuracy (Reihanisaransari et al., 2022).

Mao et al. (2022) proposed a deep neural network approach to predict the stress and strain of solder joints in printed circuit boards under various drop conditions. The model accurately predicts the mechanical responses of solder joints in BGA packaging structures with less than 10% error.

Wang et al. (2019) used a general regression neural network model to diagnose defects in solder bumps. Using images from a scanning acoustic microscope to train the model, they achieved an accuracy of 97.79%.

Sha et al. (2022) used the Histogram of Oriented Gradient (HOG) feature extraction method combined with an SVM classification model to detect defects in solder bumps used in flip chip technology, achieving a high detection accuracy of 96.96%.

ML models have also been shown to be effective in optimizing process parameters and addressing void problems in the underfill process of BGA chip packages (Ling et al., 2025; Nashrudin et al., 2022). Muhammad Naqib Nashrudin et al. (2022) proposed a neural network regression model to analyze void formation in the no-flow underfill process and achieved high prediction accuracy ($R^2 = 0.95159$, error = 0.15885), with chip placement speed identified as the most influential factor. Similarly, Ling et al. (2025) used supervised machine learning to investigate void problems in BGA chip underfill, identifying valve pressure as the primary cause of voids and achieving 88.9% accuracy.

Artificial Neural Network (ANN) models, including Recurrent Neural Networks (RNN), Long Short-Term Memory (LSTM), and Multilayer Perceptrons (MLP), provide a robust framework for predicting solder joint behavior, fatigue life, and damage under thermal cycling. These models are typically trained using data sets generated by validated FE simulations, ensuring accuracy and reliability of their predictions. These approaches increase computational efficiency and reduce reliance on experimental testing. Machine learning capabilities to handle complex, nonlinear data sets, coupled with model calibration techniques such as Bayesian inference, improve prediction accuracy by addressing uncertainties and incorporating prior knowledge (Muench et al., 2022; Ross, 2023; Tauscher et al., 2024; Yuan & Lee 2020; Yuan et al., 2021).

The literature shows that different ML models can have different levels of performance when applied to similar problems. Existing studies on electronic packaging reliability using ML models are limited to temperature cycling or classification models to detect defects in solder bumps. In particular, there is a significant gap in the current research as very few studies have investigated the application of ensemble methods to evaluate the reliability of solder joints under drop impact conditions. This study highlights the capabilities of ensemble methods, which demonstrate accurate predictive performance with moderate data sets.

This study presents a comprehensive approach to predict solder joint failure in PCBA packaging structures using ensemble methods. FE simulations were performed using ABAQUS and validated against experimental drop tests by correlating the dynamic responses of the PCBA during impact. Since solder joint failure is primarily attributed to the development of peel stress in solder balls during drop impact (Gu et al., 2017; Luan et al., 2006), this study focuses on evaluating and predicting the peel stress induced in solder joints as a key metric for failure assessment. Parametric studies conducted on various design factors of the PCBA identified PCB modulus, thickness, solder ball diameter and solder ball material as the major contributory factors affecting the stress distribution in the solder joints (Yagnamurthy & Nathi, 2025). These contributing parameters were systematically varied and the resulting dynamic responses from FE simulations were used to generate a dataset for training ML models. In this study, ensemble methods such as Random Forest regression, Extra tress regression, and XG Boost regression models were used to predict the dynamic responses of the PCBA under drop impact conditions. Because the peel stress during the drop event is influenced by nonlinear material deformation and geometric interactions, ensemble models are well suited to capture these nonlinear, multivariate relationships. These models allow for faster design iteration and optimization, enabling parametric studies while reducing computational costs and accelerating the development of robust packaging structures. Thus, the study highlights the potential of ML models to replace traditional FE simulations, offering significantly improved efficiency while maintaining high prediction accuracy.

2. MATERIALS AND METHODS

2.1. Drop test experiments

To evaluate the dynamic response of the PCBA, drop tests were performed in accordance with JESD22-B111A using a Lansmont P-30 shock tower. Fig. 1(a). shows the schematic diagram of the PCBA, while Fig. 1(b). shows the solder ball array of the package. A 100×100×1 mm PCB with a centrally mounted BGA package facing down was mounted on a 135×135×25 mm baseplate using four 3.1 mm diameter standoffs. The base plate was then secured to the drop table as shown in Figure 1(c). The drop heights were adjusted to produce a 1500G peak half-sine pulse acceleration for 0.5 ms duration, in accordance with Service Condition B of the JESD22-B111A standard. A single-axis accelerometer was mounted on the baseplate to measure the impact pulse, and two rectangular strain gauge rosettes were placed on the PCB closer to the package to capture the longitudinal strain during the drop, as shown in Figure 1(c). The shock pulse measured by the accelerometer during the drop event is shown in Figure 1(d). Longitudinal strain and acceleration were recorded during the drop using a high-speed DAQ system.

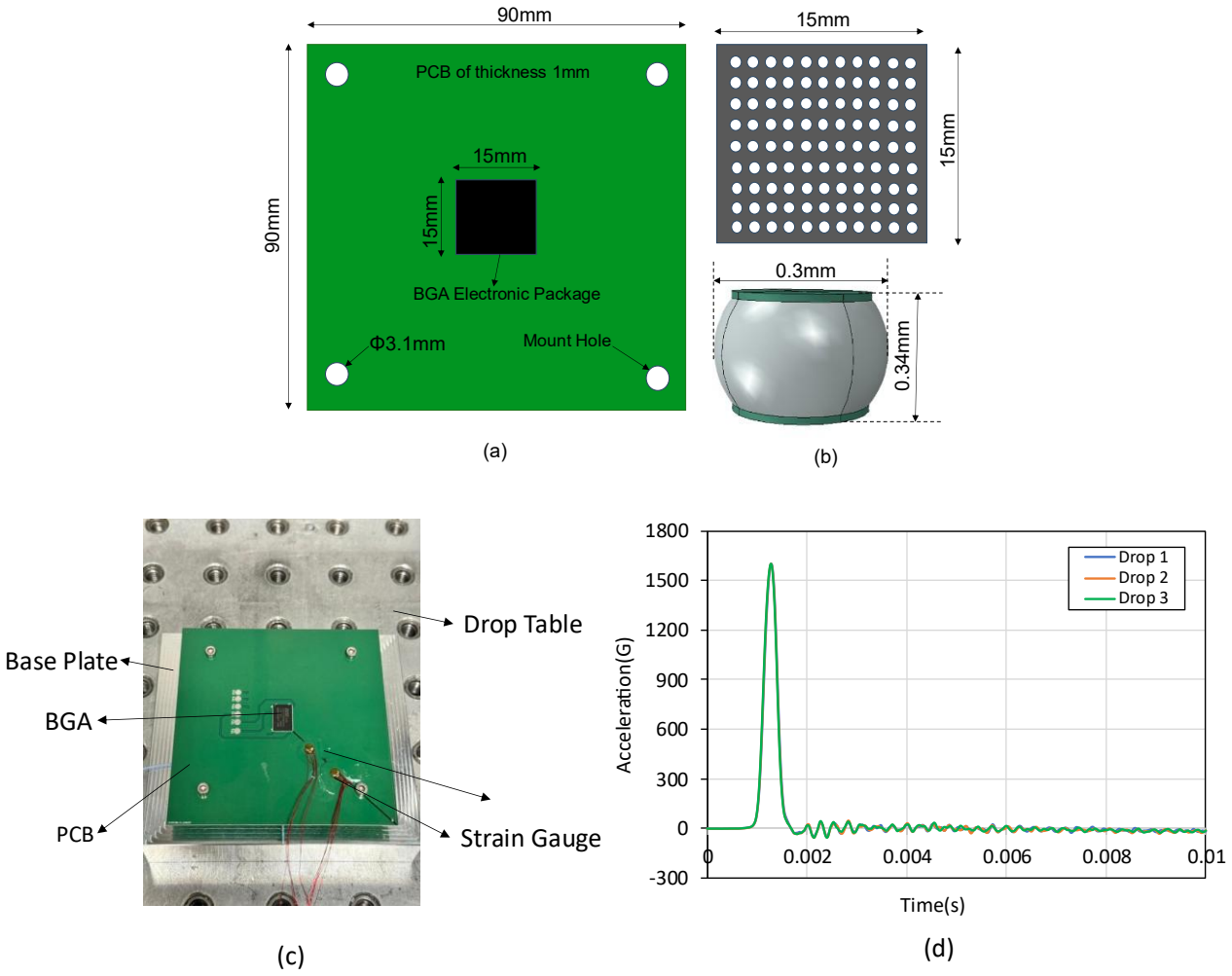

Fig. 1. a) Schematic of PCBA (b) BGA package and Solder Ball (c) Test Board (d) Acceleration pulse for 1500G

2.2. Finite element methods

A dynamic explicit analysis of the PCBA was performed using Abaqus to obtain the maximum peel stress and longitudinal strain in the critical solder ball during the drop impact event. A finite element model of the PCB with the BGA package mounted in the center is shown in Figure 2. The model includes a printed circuit board (PCB) with a thickness of 1 mm and an elastic modulus of 30 GPa. Solder balls with a diameter of 0.3 mm, an elastic modulus of 35.7 GPa, and a pitch of 0.8 mm are included in the assembly. Due to the symmetry

of the assembly, only a quarter model was considered for the simulation to reduce the computation time. The dimensions and material properties of the components of the assembly are listed in Table. 1. The model was meshed using C3D8R (8-node linear brick) elements with 148,610 nodes and 108,622 elements. Input-G method was used to simulate the model, with an acceleration of 1500g applied directly to the mounting holes in the form of a half-sine wave with an impact duration of 0.5ms.

Parametric studies conducted to optimize the design factors of the PCBA revealed that PCB thickness, PCB modulus, solder ball diameter and solder ball material significantly influence the stress distribution in the critical solder joints during the drop events compared to the substrate and die properties (Yagnamurthy & Nathi, 2025). Simulations were performed by varying board thickness (0.8-1.5mm), board modulus (20-30GPa), solder ball diameter in the range (0.2-0.5mm), along with two solder ball materials SAC105 (Sn-1.0Ag-0.5Cu) and SAC1205N (Sn-1.2Ag-0.5Cu with nickel). A total of 250 simulation results were generated and used as a dataset to train and validate the ML models.

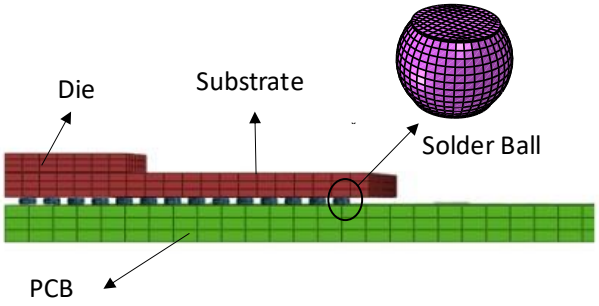

Fig. 2. Finite Element Model of Quarter PCBA

Tab. 1. Dimensions and material properties of PCBA components

Component	Dimension (mm)	Youngs Modulus (GPa)	Poisson Ratio	Density (kg/m^3)
PCB	100x100x1	30	0.3	1780
Solder Ball (SAC105)	ϕ 0.3	35.7	0.3	7300
Solder ball (SAC1205N)	ϕ 0.3	39.8	0.3	7500
Copper Pad	ϕ0.3, 0.02thick	130	0.3	8830
Substrate	0.75	30	0.3	1780
Underfill	0.02	20	0.3	1500
Die	0.5	160	0.3	2230

2.3. Mesh sensitivity analysis

Since the smallest mesh elements were in the solder balls, a mesh sensitivity analysis was performed by varying their mesh size to determine the optimal balance between simulation accuracy and computational efficiency. Figure 3 illustrates the variation of peel stress results for different solder ball mesh sizes. A finer mesh increases the number of nodes per unit area or volume, which improves the accuracy of the stress and deformation representation. The analysis tested element sizes of 0.04, 0.05, 0.06, 0.08, 0.1, and 0.12 mm. It was observed that beyond a certain mesh size, the results begin to converge and become largely independent of further mesh refinement. This convergence was observed from a mesh size of 0.06 mm, corresponding to approximately 75,000 elements. As a result, an optimal mesh size of 0.04 mm was selected with a total of 110,456 elements. This configuration achieved convergence, required a simulation time of 2,800 seconds, and produced a maximum peel stress of 162.12 MPa.

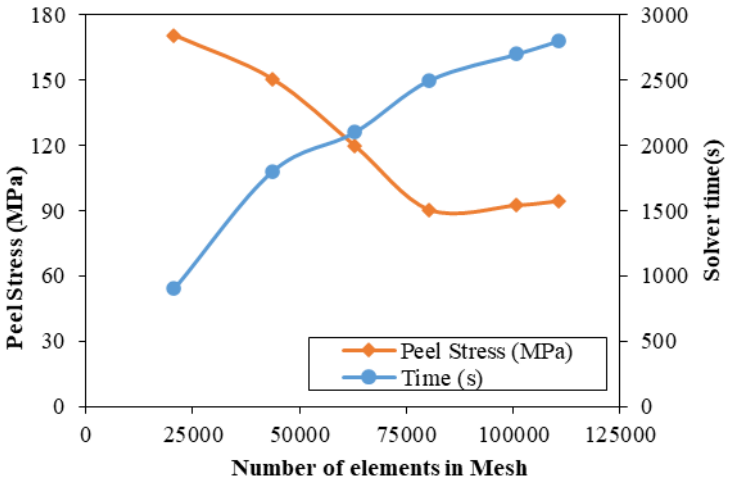

Fig. 3. Mesh sensitivity

3. PREDICTIVE MODEL BASED ON ENSEMBLE METHODS

Since the drop simulation is a dynamic event, the peel stress in solder joints is strongly influenced by nonlinear material behavior and geometric interactions. Ensemble models effectively capture complex nonlinear and multivariate relationships without prior assumptions, and they generalize well when applied to moderate-sized datasets (Chen & Guestrin, 2016).Therefore, in this study, ensemble methods were chosen to predict the peel stress in the critical solder joint. Extra Trees reduces overfitting by averaging multiple randomized decision trees, while Random Forest uses bagging to accomplish the same. XGBoost minimizes both bias and variance through boosting and regularization (Bentéjac et al., 2021). Eighty percent of the simulation data was used for training, and the remaining 20% was reserved for testing. The test data was evaluated using ten randomized validation cycles to ensure robustness. The regression models were implemented using Python programming. Figure 4 illustrates the research methodology.

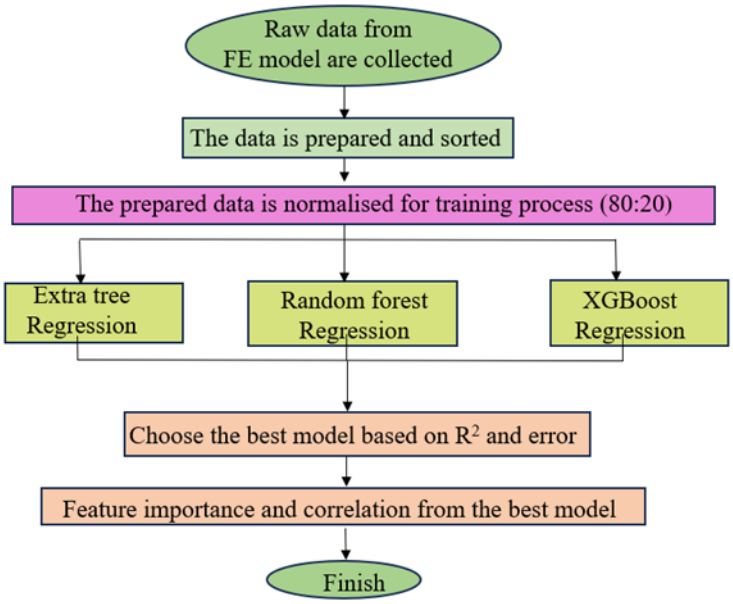

Fig. 4. Flowchart of the study

3.1. Random forest regression

Random forest is an ensemble learning algorithm that constructs multiple decision trees using different subsets of the data and combines their predictions to improve accuracy and reduce overfitting (Wang & Wang, 2020). Each tree is trained on a different random subset of the data using bootstrap sampling, and each split considers only a random set of features. This reduces the similarity between trees and improves the model's ability to generalize. Figure 5(a). shows the graphical representation of Random Forest regression. By aggregating multiple decision trees, Random Forest mitigates the risk of overfitting that a single deep tree might face, resulting in a more robust and reliable model. Increasing the number of trees increases stability and further improves predictive performance, making random forest a widely used tool in machine learning (Shehadeh et al., 2021).

3.2. Extra tree regression

Extra Trees regression is an extension of the Random Forest algorithm designed to improve predictive performance while reducing the risk of overfitting. Extra Trees uses an ensemble of decision trees and uses random feature selection to improve model generalization. However, it randomly selects both the feature and its split value based on the optimization criterion. This additional randomness increases the variance of the model while maintaining strong predictive accuracy (Ahmad et al., 2018). A graphical representation of the Extra Trees regression is shown in Figure 5(b).

3.3. XGBoost regression

XGBoost regression is a powerful and scalable ML algorithm widely used for regression and classification tasksthatoutperforms Random Forest and Extra Trees, running more than 10 times faster on a single machine while efficiently handling large datasets in distributed and memory-constrained environments (Bentéjac et al., 2021). XGBoost builds an ensemble of decision trees sequentially, with each new tree correcting the errors of the previous trees, as shown inFigure 5(c). It uses gradient boosting principles while incorporating key optimizations such as regularization to prevent overfitting, shrinkage to control learning rates, and parallel processing for increased efficiency. These features make XGBoost effective for managing large datasets, capturing complex relationships, and handling high-dimensional data while maintaining exceptional predictive accuracy (Huang et al., 2021).

In order to evaluate the effectiveness of the regression models mentioned above, several mathematical evaluation metrics were calculated. These metrics include Mean Absolute Error (MAE), Root Mean Squared Error (RMSE), and Coefficient of Determination (R2). MAE is a metric commonly used in regression analysis to measure the accuracy of a predictive model. It calculates the average of the absolute differences between the predicted and actual values from the data set. Here, m is the total number of observations, Xi is the predicted value for theith data point, and Yi is the actual value of theith data point. Equation 1 illustrates the calculation of the MAE (Chen & Guestrin, 2016).

$$\mathrm{MAE} = \frac{1}{\mathrm{m}}\sum_{\mathrm{i}=1}^{\mathrm{m}} |\mathrm{X_i} - \mathrm{Y_i}| \tag{1}$$

Equation (2) displays the RMSE, which is the root mean square difference between the actual and predicted values, while Equation (3) displays the coefficient of determination,R2, which can be interpreted as the proportion of the variance in the dependent variable that can be predicted from the independent variables (Chicco et al., 2021).

$$\mathrm{RMSE} = \sqrt{\frac{1}{\mathrm{m}}\sum_{\mathrm{i}=1}^{\mathrm{m}}(\mathrm{X_i} - \mathrm{Y_i})^2} \tag{2}$$

The optimal model is identified by its high predictive accuracy and low error.

$$\mathrm{R}^2 = 1 - \frac{\sum_{\mathrm{i}=1}^{\mathrm{m}}(\mathrm{X_i}-\mathrm{Y_i})^2}{\sum_{\mathrm{i}=1}^{\mathrm{m}}(\bar{\mathrm{Y}}-\mathrm{Y_i})^2} \tag{3}$$

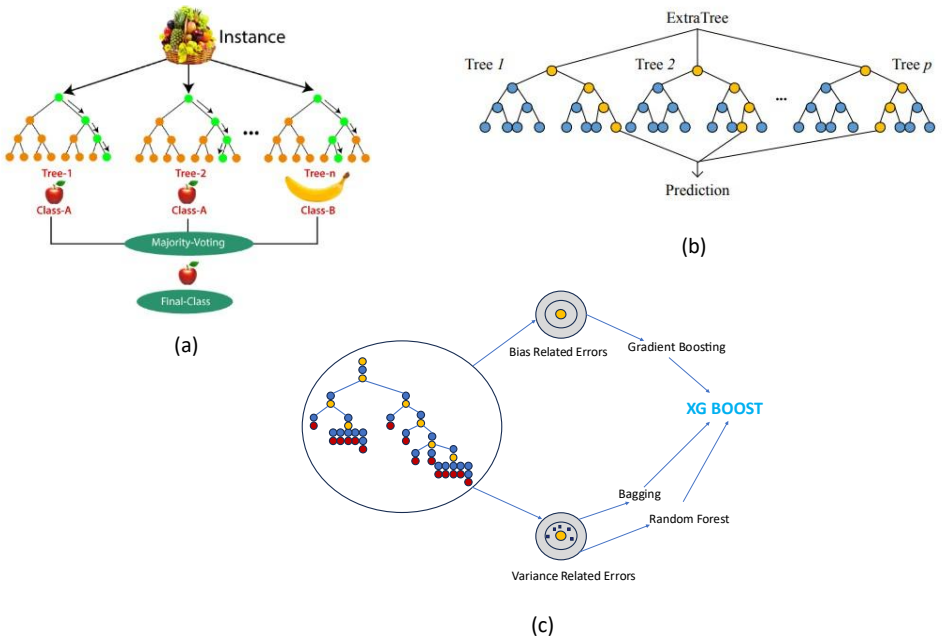

Fig. 5. Structural overview of regression models: (a) Random forest regression (b) Extra tree regression (c) XGBoost regression (Ahmad et al., 2018; Chakraborty et al., 2022; Huang et al., 2021; Shehadeh et al., 2021)

4. RESULTS AND DISCUSSION

4.1. Finite element simulation

The simulation results show that the maximum peel stress occurs at the interface between the PCB and the solder joint, in the cornermost solder ball closer to the PCB mounting hole. Figure 6. shows the peel stress (S33) and longitudinal strain (LE11) in the most critical solder ball for both SAC105 and SAC1205N. The peel stress for SAC105 is 164.8 MPa, while that for SAC1205N is 138.3 MPa. Similarly, the longitudinal strain is 1360 microstrain for SAC105 and 837 microstrain for SAC1205N.

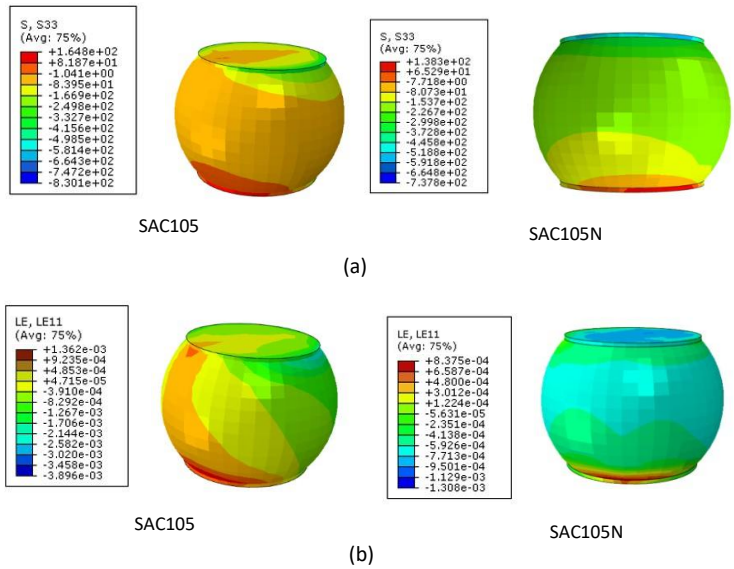

Fig. 6. (a) Peel stress in the most critical solder joint of SAC105 and SAC1205N (b) Longitudinal Strain (LE33) in the most critical solder joint of SAC105 and SAC1205N

Figure 7. shows the variation of peel stress for SAC105 and SAC1205N solder joints under different design parameters: PCB modulus, PCB thickness and solder ball diameter. Figure 7(a). shows that increasing the PCB

modulus reduces the peel stress in the critical solder joint for both SAC105 and SAC1205N. The maximum stress of 266.5MPa for SAC105 and 210.4MPa for SAC1205N occurs at the lowest modulus of 7.5GPa, with the stress decreasing more gradually and linearly above 30GPa. A stiffer board improves solder joint reliability by minimizing peel stress and resisting dynamic deformation. Figure 7(b). shows that peel stress decreases with increasing board thickness, from 253.9MPa to 57.7MPa for SAC105 and from 201.5MPa to 87MPa for SAC1205N. Figure 7(c). shows that larger solder ball diameters result in lower peel stress. The smallest diameter, 0.075mm, results in maximum stress (270.47MPa for SAC105, 210.45MPa for SAC1205N), which decreases significantly to 56.15MPa and 42.34MPa, respectively, for a solder ball diameter of 0.9mm. Larger diameter improves contact area and mechanical strength, which reduces shock-induced stress.

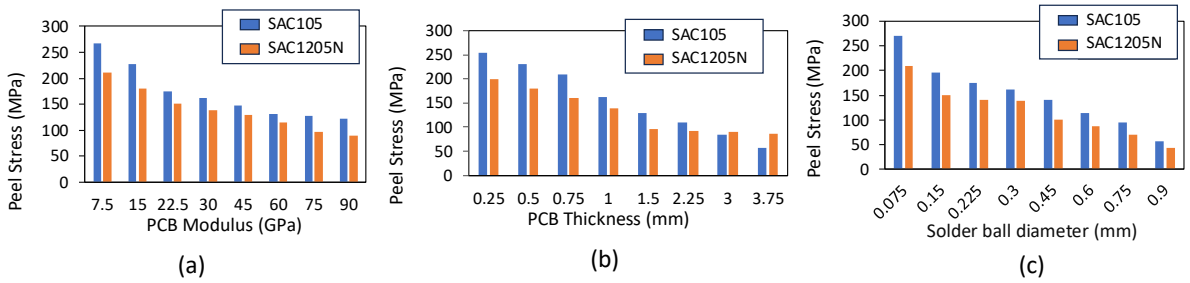

Fig. 7. (a) Peel stress variation versus variation of the PCB Modulus while PCB thickness is 1mm and solder ball diameter is 0.3mm (b) Peel Stress variation versus PCB thickness while PCB modulus is 30GPa and solder ball diameter is 0.3mm (c) Peel stress variation vs Solder ball diameter while PCB modulus is 30GPa and PCB thickness is 1mm

4.2. Experimental validation

Drop test experiments measured the longitudinal strain in the critical solder joint using a strain gauge mounted on the PCB closer to the BGA package. To ensure repeatability, each experiment was performed under identical conditions for three consecutive drops from the same height. The dynamic strain obtained from the simulations is validated against the experimental results. Figure 8. shows a good correlation between the experimental and simulated longitudinal strain during drop impact for both solder materials. A positive peak in the dynamic strain along the longitudinal direction of the board indicates upward bending, while a negative peak indicates downward bending. The amplitude of PCB bending gradually decreases over time.

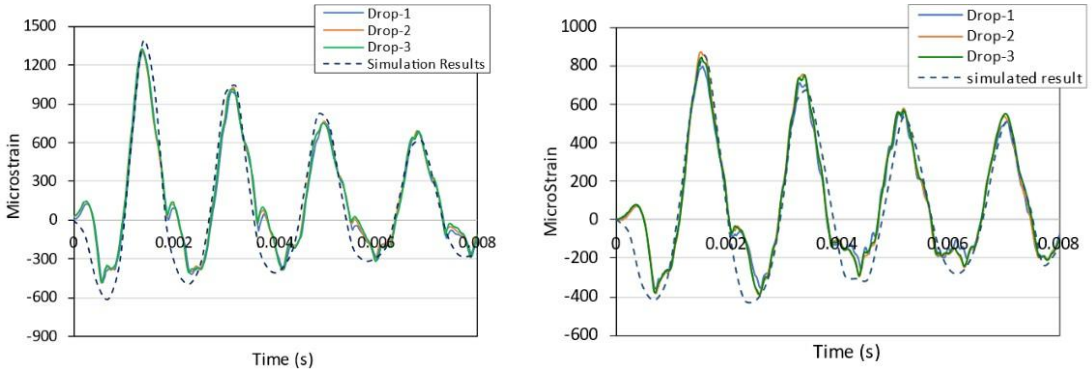

Fig. 8. Comparison of experimental and simulated longitudinal strain in (a) SAC105 solder joint (b) SAC1205N solder joint

4.3 Predictive model based on ensemble methods

After validating the FE simulations with experimental results, an ML-based predictive model was developed using three ensemble methods: Extra Trees regression, Random Forest regression, and XGBoost regression. The models were trained on data generated by varying the contributing parameters that influence peel stress.

Trend lines comparing peel stress from FE simulations and predictive models are plotted. Each regression produced a unique peel stress prediction that influenced the trend and slope. Regression methods demonstrated strong predictive capabilities for continuous variables such as peel stress. The regression line indicates that the

data points in Figure 9(a) are more out of line with the trend line, while Figure 9(b) and Figure 9(c) are more closely aligned, indicating that all three models generalize well across different combinations of PCB parameters.

Model prediction accuracy was evaluated using MAE and RMSE as performance metrics. However, evaluating regression model performance using these metrics alone can be misleading, as each captures different aspects of prediction error and does not provide a complete picture of model effectiveness (Chicco et al., 2021). Therefore, R^2 values were also considered. R^2 represents the proportion of variance in the dependent variable explained by the model, while MAE and RMSE reflect the size and distribution of the prediction errors. The model with the highest R^2 was selected as the optimal model. An R^2 value between 0 and 1 indicates partial prediction of the outcome, while a value of 1 indicates perfect prediction (Rengasamy et al., 2022). Tab. 2 presents the interpretation of the R^2 values. A higher R^2 indicates a stronger correlation between predicted and actual values, demonstrating the effectiveness of the model in explaining the observed variation (Chen & Guestrin, 2016).

Tab. 3 presents the performance metrics of the three regression models. The XGBoost regression achieved the highest R^2 value of 0.9606, along with the lowest error metrics, with MAE and RMSE values of 8.89 and 13.79, respectively. The Random Forest regression model achieved an R^2 value of 0.950, with MAE and RMSE values of 11.55 and 14.17, respectively. The Extra Trees regression achieved an R^2 of 0.945, with MAE and RMSE of 10.39 and 16.60, respectively. These results indicate that all three regression models have high predictive accuracy, with R^2 values above 0.94. Among them, XGBoost showed the best performance with the highest R^2 and the lowest prediction errors, making it the most suitable for accurate data prediction.

Tab. 2. Interpretation of coefficient determination (Chen & Guestrin, 2016)

R^2 Value	Interpretation
$R^2=1$	Perfect fit
$0.85 \leq R^2 < 1$	Strong fit
$0.5 \leq R^2 < 0.85$	Moderate fit
$0.2 \leq R^2 < 0.5$	Weak fit
$0.2 \leq R^2 < 0.5$	Very weak fit

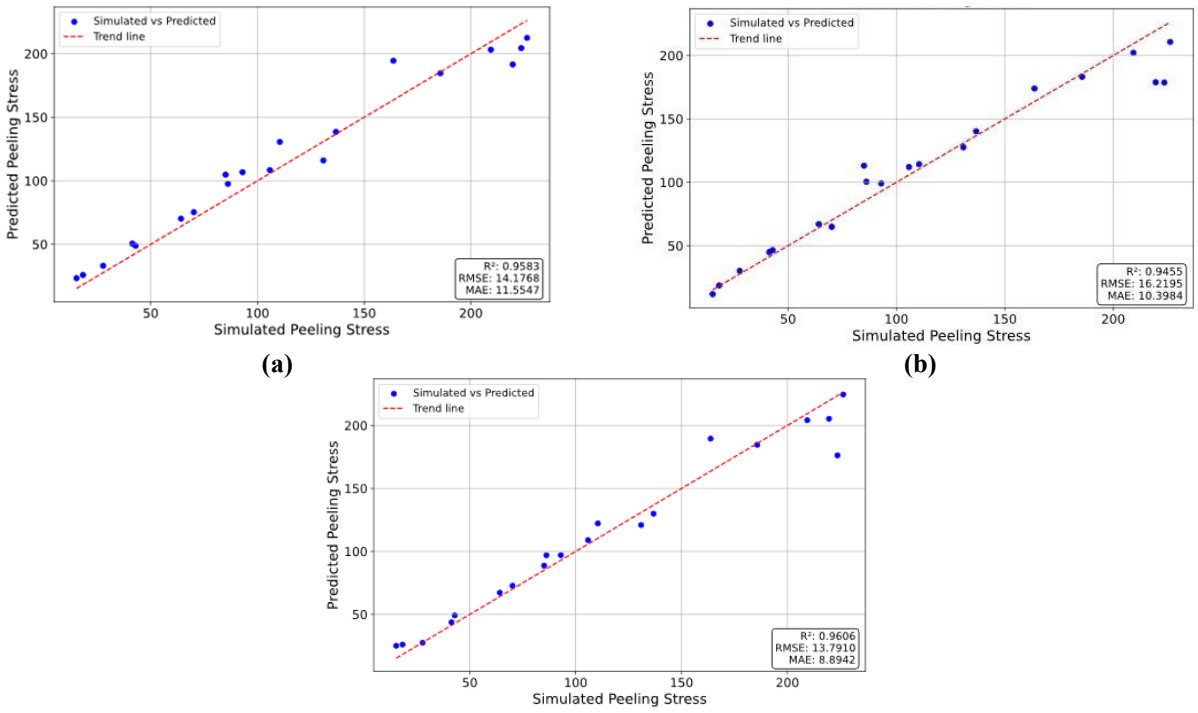

Fig. 9. Graph of predicted peeling stress vs. simulated peeling stress:
(a) Random forest regression, (b) Extra tree regression, and (c) XGBoost regression

Tab. 3. Performance metrics of different regression models

Algorithm Model	MAE	RMSE	R2
Random Forest Regression	11.5547	14.1768	0.9583
Extra trees Regression	10.3984	16.2195	0.9455
XG Boost Regression	8.8942	13.791	0.9606

4.4. Feature importance analysis

The feature importance analysis across the three regression models, shown in Figure 10, highlights the importance of each input parameter in influencing the model predictions. Solder ball material emerged as the most influential feature, with importance values ranging from 0.4475 in XGBoost (the most accurate model) to 0.4700 in Extra Trees. This was followed by PCB thickness, which ranked second, with values ranging from 0.3529 in XGBoost to 0.3899 in Random Forest. Solder ball diameter showed moderate importance, ranging from 0.1339 in XGBoost to 0.0952 in Random Forest. PCB modulus consistently ranked as the least influential feature, with importance values of 0.0657 in XGBoost and 0.0611 in Extra Trees. These rankings underscore the dominant role of solder ball material and PCB thickness in driving predictive performance, indicating their stronger influence compared to the other features analyzed.

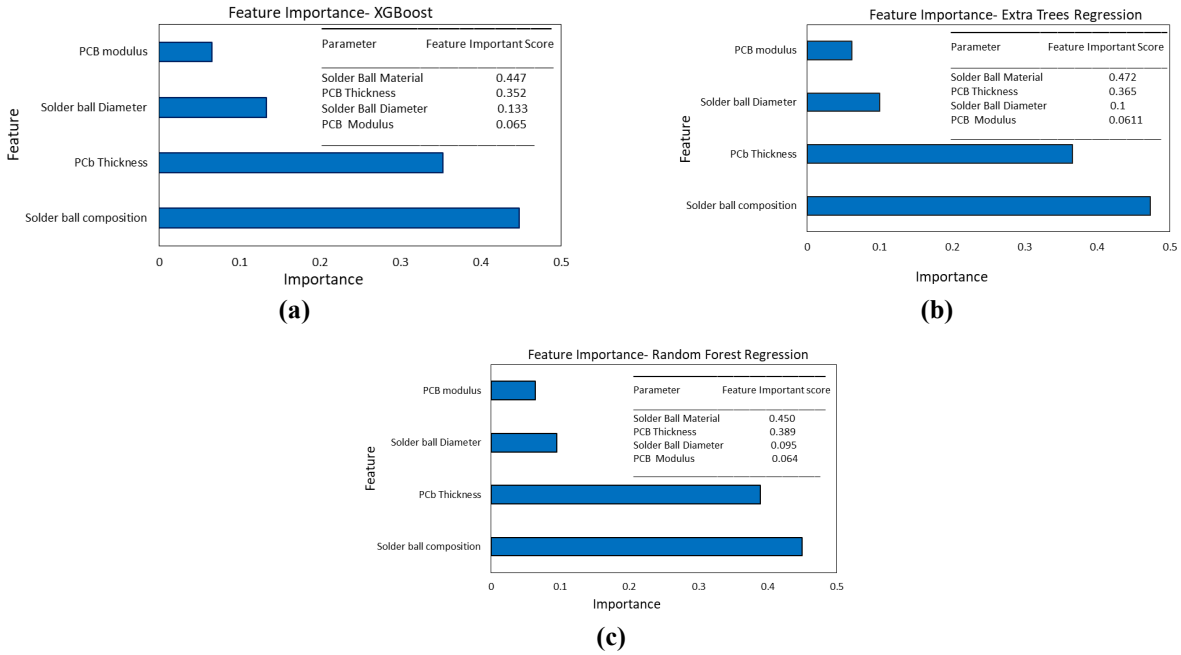

Fig. 10. Feature significance results (a) XGBoost regression (b) Extra tree regression (c) Random forest regression

4.5. Limitations of the study

The proposed approach is limited to the four dominant contributing factors, namely solder joint chemical composition, solder ball diameter, PCB thickness, and PCB modulus. The current approach can be further improved by expanding the database to include additional parameters such as solder joint geometry, solder ball pitch, substrate properties, and underfill effects. The present work relies exclusively on finite element (FE) simulations to train the predictive models. Incorporating experimental results could further improve accuracy and expand the data set. In addition, exploring alternative machine learning approaches, such as deep learning methods, may offer potential improvements in model performance.

4.6. Model evaluation and cross-validation

Figure 11. illustrates the performance of the Random Forest, Extra Trees, and XGBoost regression models at different training sample sizes for predicting solder joint peel stress. The plot highlights how each model scales with training data. The trend shows their strong learning ability even with modestly sized datasets. The

consistent performance across methods justifies the selection of ensemble methods for this study, demonstrates their strong generalization ability, and justifies their use for predicting dynamic responses for the reliability of electronic packages.

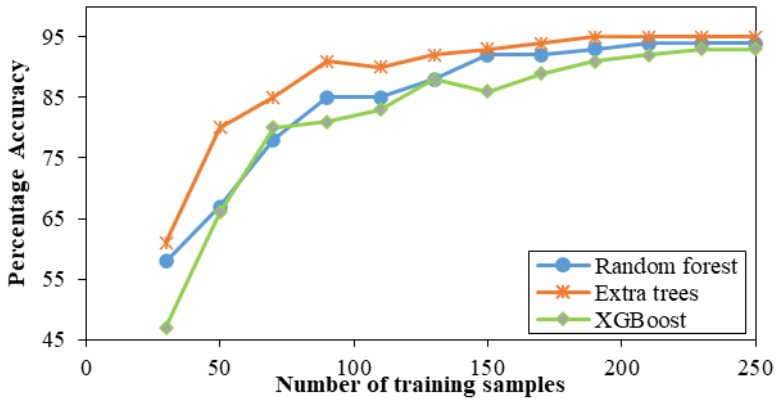

Fig. 11. Learning curves of ensemble regression models

5. CONCLUSIONS

The failure of solder joints under drop impact was analyzed by incorporating various contributing factors through FE simulations and ML models. Based on the results, the following conclusions were derived:

1. The simulation results showed a strong correlation with the experimental results and indicated that the corner-most solder ball of the BGA package on the PCB side was the most vulnerable region, experiencing the highest stress due to the differences in stiffness and material properties of the components. SAC205N outperformed SAC105, showing 16% lower peel stress (138.3 MPa vs. 164.8 MPa) and 38.5% lower strain (837 microstrain vs. 1360 microstrain) due to improved bonding from the nickel content.
2. Of the three ensemble methods evaluated (Random Forest, Extra Trees, and XGBoost Regression), all demonstrated high predictive accuracy with R^2 values greater than 0.94. The predictive models showed strong learning capabilities even with modestly sized datasets. The XGBoost regression outperformed the others in predicting peel stress during drop impact, achieving the highest R^2 value of 0.96 and the lowest error rates, with an MAE of 8.89 and RMSE of 13.79.
3. The most accurate model, XGBoost, identified solder ball material as the most influential factor with an importance value of 0.4475, followed by PCB thickness with 0.3529. Solder ball diameter showed a moderate influence with an importance value of 0.133, while PCB modulus was the least influential with an importance value of 0.065. These results emphasized the significant role of solder ball material and PCB thickness in model prediction performance.

6. FUTURE SCOPE

Future work can explore alternative predictive models, including deep learning and hybrid approaches, to capture more complex interactions. The current approach can also be further explored by expanding the database to include additional parameters such as solder ball shape, height and pitch, substrate properties, and underfill effects.

Author Contributions

Venkata Naga Chandana YAGNAMURTHY: Conceptualization, modelling and analysis, data curation, interpretation of results, original draft writing, review and editing, writing.

Venu Kumar NATHI: Data collection, Study conception, design, data collection, supervision, investigation on challenges and draft manuscript preparation, conceptualization, writing – original draft, analysis and, Data collection.

Conflicts of Interest

The authors declare that they have no conflicts of interest to this work.

REFERENCES

Ahmad, M. W., Reynolds, J., & Rezgui, Y. (2018). Predictive modelling for solar thermal energy systems: A comparison of support vector regression, random forest, extra trees and regression trees. *Journal of Cleaner Production*, *203*, 810-821. https://doi.org/10.1016/j.jclepro.2018.08.207

Apalowo, R. K., Abas, M. A., Che Ani, F., Muhamed Mukhtar, M. A. F., & Ramli, M. R. (2024). Thermal fatigue life prediction and intermetallic compound behaviour of SAC305 BGA solder joints subject to accelerated thermal cycling test. *Soldering & Surface Mount Technology*, *36*(3), 154-164. https://doi.org/10.1108/SSMT-12-2023-0075

Arriola, E. R., Ubando, A. T., Gonzaga, J. A., & Lee, C. C. (2023). Wafer-level chip-scale package lead-free solder fatigue: A critical review. *Engineering Failure Analysis*, *144*, 106986. https://doi.org/10.1016/j.engfailanal.2022.106986

Bentéjac, C., Csörgő, A., & Martínez-Muñoz, G. (2021). A comparative analysis of gradient boosting algorithms. *Artificial Intelligence Review*, *54*, 1937-1967. ttps://doi.org/10.1007/s10462-020-09896-5

Chakraborty, P., Rafiammal, S. S., Tharini, C., & Jamal, D. N. (2022). Influence of bias and variance in selection of machine learning classifiers for biomedical applications. *Smart Data Intelligence (ICSMDI)* (pp. 459-472). Springer Nature. https://doi.org/10.1007/978-981-19-3311-0_39

Chen, T., & Guestrin, C. (2016). Boost: A scalable tree boosting system. *22nd ACM SIGKDD International Conference on Knowledge Discovery and Data Mining* (pp. 785-794). Association for Computing Machinery. https://doi.org/10.1145/2939672.2939785

Chen, Y., Jing, B., Li, J., Jiao, X., Hu, J., & Wang, Y. (2020). Failure analysis and modeling of solder joints in BGA packaged electronic chips. *IEEE Transactions on Components, Packaging and Manufacturing Technology*, *11*(1), 43-50. https://doi.org/10.1109/TCPMT.2020.3040757

Chicco, D., Warrens, M. J., & Jurman, G. (2021). The coefficient of determination R-squared is more informative than SMAPE, MAE, MAPE, MSE and RMSE in regression analysis evaluation. *PeerJ Computer Science*, *7*, e623. https://doi.org/10.7717/peerj-cs.623

Gu, J., Lei, Y., Lin, J., Fu, H., & Wu, Z. (2017). The failure models of lead-free Sn-3.0 Ag-0.5 Cu solder joint reliability under low-G and high-G drop impact. *Journal of Electronic Materials*, *46*, 1396-1404. https://doi.org/10.1007/s11664-016-5027-y

Gu, J., Lin, J., Lei, Y., & Fu, H. (2018). Experimental analysis of Sn-3.0 Ag-0.5 Cu solder joint board-level drop/vibration impact failure models after thermal/isothermal cycling. *Microelectronics Reliability*, *80*, 29-36. https://doi.org/10.1016/j.microrel.2017.10.014

Huang, J. S., Liew, J. X., Ademiloye, A. S., & Liew, K. M. (2021). Artificial intelligence in materials modeling and design. *Archives of Computational Methods in Engineering*, *28*, 3399-3413. https://doi.org/10.1007/s11831-020-09506-1

JEDEC. (2024, June). *Board level drop test method of components for handheld electronic products. JESD22-B111A*. https://www.jedec.org/standards-documents/docs/jesd-22-b111

Ling, C., Azahari, T., Abas, M. A., & Ng, F. C. (2025). Correlation study on voiding in underfill of large quantity ball grid array chip using machine learning. *Journal of Electronic Packaging*, *147*(1), 011001. https://doi.org/10.1115/1.4065077

Luan, J. E., Tee, T. Y., Pek, E., Lim, C. T., Zhong, Z., & Zhou, J. (2006). Advanced numerical and experimental techniques for analysis of dynamic responses and solder joint reliability during drop impact. *IEEE Transactions on Components and Packaging technologies*, *29*(3), 449-456. https://doi.org/10.1109/TCAPT.2006.880455

Mao, M., Wang, W., Lu, C., Jia, F., & Long, X. (2022). Machine learning for board-level drop response of BGA packaging structure. *Microelectronics Reliability*, *134*, 114553. https://doi.org/10.1016/j.microrel.2022.114553

Muthuram, N., & Saravanan, S. (2022). Free fall drop impact analysis of board level electronic packages. *Microelectronics Journal*, *129*, 105601. https://doi.org/10.1016/j.mejo.2022.105601

Muench, S., Bhat, D., Heindel, L., Hantschke, P., Roellig, M., & Kaestner, M. (2022). Performance assessment of different machine learning algorithm for life-time prediction of solder joints based on synthetic data. *23rd International Conference on Thermal, Mechanical and Multi-Physics Simulation and Experiments in Microelectronics and Microsystems (EuroSimE)* (pp. 1-10). IEEE. https://doi.org/10.1109/EuroSimE54907.2022.9758919

Niu, X. Y., Li, W., Wang, G. X., & Shu, X. F. (2015). Effects of temperature and strain rate on mechanical behavior of low-silver lead-free solder under drop impact. *Journal of Materials Science: Materials in Electronics*, *26*, 601-607. https://doi.org/10.1007/s10854-014-2441-x

Nashrudin, M. N., Ng, F. C., Abas, A., Abdullah, M. Z., Ali, M. Y. T., & Samsudin, Z. (2022). Prediction of the void formation in no-flow underfill process using machine learning-based algorithm. *Microelectronics Reliability*, *135*, 114586. https://doi.org/10.1016/j.microrel.2022.114586

Porathur, F. J., Kamble, V. G., Stadler, E., Huber, F., Gruber, D. P., & Fuchs, P. F. (2024). Warpage optimization of package substrates using metamodels: A review. *25th International Conference on Thermal, Mechanical and Multi-Physics Simulation and Experiments in Microelectronics and Microsystems (EuroSimE)* (pp. 1-9). IEEE. https://doi.org/10.1109/EuroSimE60745.2024.10491528

Reihanisaransari, R., Samadifam, F., Salameh, A. A., Mohammadiazar, F., Amiri, N., & Channumsin, S. (2022). Reliability characterization of solder joints in electronic systems through a neural network aided approach. *IEEE Access*, *10*, 123757-123768. https://doi.org/10.1109/ACCESS.2022.3224008

Ross, J. S. (2023). Comparing the performance of different machine learning models in the evaluation of solder joint fatigue life under thermal cycling. *Portland State University*. https://doi.org/10.15760/etd.3425

Rengasamy, D., Mase, J. M., Kumar, A., Rothwell, B., Torres, M. T., Alexander, M. R., Winkler, D. A., & Figueredo, G. P. (2022). Feature importance in machine learning models: A fuzzy information fusion approach. *Neurocomputing*, *511*, 163-174. https://doi.org/10.1016/j.neucom.2022.09.053

Sha, Y., He, Z., Du, J., Zhu, Z., & Lu, X. (2022). Intelligent detection technology of flip chip based on H-SVM algorithm. *Engineering Failure Analysis*, *134*, 106032. https://doi.org/10.1016/j.engfailanal.2022.106032

Shehadeh, A., Alshboul, O., Al Mamlook, R. E., & Hamedat, O. (2021). Machine learning models for predicting the residual value of heavy construction equipment: An evaluation of modified decision tree, LightGBM, and XGBoost regression. *Automation in Construction*, *129*, 103827. https://doi.org/10.1016/j.autcon.2021.103827

Tee, T. Y., Ng, H. S., Lim, C. T., Pek, E., & Zhong, Z. (2004). Impact life prediction modeling of TFBGA packages under board level drop test. *Microelectronics Reliability*, *44*(7), 1131-1142. https://doi.org/10.1016/j.microrel.2004.03.005

Tauscher, M., Lämmle, S., Roos, D., & Wilde, J. (2024). Bayesian calibration of ball grid array lifetime models for solder fatigue. *Microelectronics Reliability*, *155*, 115366. https://doi.org/10.1016/j.microrel.2024.115366

Wang, P. H., Lee, Y. C., Lee, C. K., Chang, H. H., & Chiang, K. N. (2021). Solder joint reliability assessment and pad size studies of FO-WLP with glass substrate. *IEEE Transactions on Device and Materials Reliability*, *21*(1), 96-101. https://doi.org/10.1109/TDMR.2021.3056054

Wang, S., & Wang, Y. (2020). Improving random forest algorithm by Lasso method. *Journal of Statistical Computation and Simulation, 91*(2), 353-367. https://doi.org/10.1080/00949655.2020.1814776

Wang, Z., Liu, X., He, Z., Su, L., & Lu, X. (2019). Intelligent detection of flip chip with the scanning acoustic microscopy and the general regression neural network. *Microelectronic Engineering*, *217*, 111127. https://doi.org/10.1016/j.mee.2019.111127

Wu, M. L., & Lan, J. S. (2018). Reliability and failure analysis of SAC 105 and SAC 1205N lead-free solder alloys during drop test events. *Microelectronics Reliability*, *80*, 213-222. https://doi.org/10.1016/j.microrel.2017.12.013

Xia, J., Li, G., Li, B., Cheng, L., & Zhou, B. (2017). Fatigue life prediction of package-on-package stacking assembly under random vibration loading. *Microelectronics Reliability*, *71*, 111-118. https://doi.org/10.1016/j.microrel.2017.03.005

Yagnamurthy, V. N. C., & Nathi, V. K. (2025). Board level solder joint analysis of ball grid array package under drop test using finite element methods. *Matéria (Rio de Janeiro)*, *30*, e20240798. https://doi.org/10.1590/1517-7076-RMAT-2024-0798

Yuan, C., Fan, X., & Zhang, G. (2021). Solder joint reliability risk estimation by AI-assisted simulation framework with genetic algorithm to optimize the initial parameters for AI models. *Materials*, *14*(17), 4835. https://doi.org/10.3390/ma14174835

Yuan, C., de Jong, S. M., & van Driel, W. D. (2024). AI-assisted design for reliability: Review and perspectives. *25th International Conference on Thermal, Mechanical and Multi-Physics Simulation and Experiments in Microelectronics and Microsystems (EuroSimE)* (pp. 1-12). IEEE. https://doi.org/10.1109/EuroSimE60745.2024.10491447

Yuan, C. C., & Lee, C. C. (2020). Solder joint reliability modeling by sequential artificial neural network for glass wafer level chip scale package. *IEEE Access*, *8*, 143494-143501. https://doi.org/10.1109/ACCESS.2020.3014156